

In-vessel Downstream Effect Tests for the APR1400

Revision 1

Non-Proprietary

July 2015

Copyright © 2015

**Korea Electric Power Corporation &
Korea Hydro & Nuclear Power Co., Ltd
All Rights Reserved**

REVISION HISTORY

Revision	Date	Page	Description
0	December 2014	All	First Issue
1	July 2015	App. A	Revised completely using the test result

This document was prepared for the design certification application to the U.S. Nuclear Regulatory Commission and contains technological information that constitutes intellectual property.

Copying, using, or distributing the information in this document in whole or in part is permitted only by the U.S. Nuclear Regulatory Commission and its contractors for the purpose of reviewing design certification application materials. Other uses are strictly prohibited without the written permission of Korea Electric Power Corporation and Korea Hydro & Nuclear Power Co., Ltd.

ABSTRACT

The APR1400 is an advanced reactor design that takes advantage of the lessons learned from operating plants and on industry trends related to the resolution of the generic safety issue (GSI)-191, including the exclusion of fibrous materials within the zone of influence of high energy line breaks. In addition, in-vessel downstream effect tests were performed to address GSI-191 considering latent fibrous materials present in the containment.

This report provides the test results of pressure drops through loss-of-coolant accident (LOCA)-generated debris deposited on a mock-up fuel assembly of the APR1400. Four tests were run to evaluate hot-leg break conditions with a four safety injection (SI) flow rate varying particle to fiber (P/F) ratios of []^{TS} Seven tests were run to evaluate cold-leg break conditions with a core boil-off rate at 700 seconds after a LOCA with varying P/F ratios of []^{TS} Two types of tests under a two SI flow rate were performed to evaluate a hot-leg break with reduced SI condition and a cold-leg break after a hot-leg switchover operation condition.

The test results on the pressure drops were compared with the available driving head in each LOCA scenario. All test results showed that the pressure drops in the mock-up fuel assembly were less than the available driving head. Therefore, sufficient driving force is available to maintain an adequate flow rate to remove decay heat; thus the long-term core cooling capability can be adequately maintained in the APR1400.

This report also includes four appendices on the effect of a flow channel gap change, the effect of debris settling, the accuracy of the GF630 flow meter, and the effect of bubbles impinging on the bottom nozzle in response to the NOV 99901453/2014-201-01(a), NOV 99901453/2014-201-01(b), NOV 99901453/2014-201-03, and NOV 99901453/2014-201-04(b), respectively.

TABLE OF CONTENTS

1	INTRODUCTION	1
2	TEST FACILITY	2
2.1	Test Column.....	2
2.2	Mixing Tank System.....	2
2.3	Circulation System.....	2
2.4	Control and Monitoring System	2
3	TEST CONDITION	6
3.1	Flow Rates	6
3.1.1	Hot-leg Break.....	6
3.1.2	Cold-leg Break	6
3.1.3	Cold-leg Break after a Hot-leg Switchover	6
3.2	Water Chemistry and Temperature.....	6
3.3	Debris Description	6
3.3.1	Particulate Debris	6
3.3.2	Fibrous Debris	7
3.3.3	Chemical Precipitates	7
3.4	Acceptance Bases for the Pressure Drop	7
3.5	Test Matrix	8
4	TEST PROCEDURE.....	12
4.1	Particulate Addition	12
4.2	Fiber Addition.....	12
4.3	Chemical Addition	12
5	TEST RESULTS	13
5.1	Hot-leg Break Tests	14
5.1.1	Summary of Hot-leg Break Tests.....	14
5.2	Cold-leg Break Tests	40
5.2.1	Summary of Cold-leg Break Tests.....	40

TS

TS

		TS
5.3	Cold-leg Break after a HLSO Test	76
5.3.1	Summary of Cold-leg Break after a HLSO Test.....	76 TS
6	QUALITY ASSURANCE.....	82
7	CONCLUSION	83
8	REFERENCES	84
	APPENDIX A EFFECT OF A FLOW CHANNEL GAP CHANGE	A-1
	APPENDIX B EFFECT OF DEBRIS SETTLING	B-1
	APPENDIX C ACCURACY OF THE GF630 FLOW METER	C-1
	APPENDIX D EFFECT OF BUBBLES IMPINGING ON THE BOTTOM NOZZLE	D-1

LIST OF TABLES

Table 2-1	Accuracy of the Measurement Instruments	3
Table 3-1	Flow Conditions in each LOCA Scenario.....	9
Table 3-2	Debris Types and Amounts per Fuel Assembly (FA)	9
Table 3-3	Fiber Length Distribution in Values	9
Table 3-4	Available Driving Heads in each LOCA Scenario	10
Table 3-5	Test Matrix.....	10
Table 5-1	Summary of the Test Results	13

TS

LIST OF FIGURES

Figure 2-1	Schematic Diagram of the Test Facility.....	4
Figure 2-2	Test Facility for the In-vessel Downstream Effect.....	5
Figure 3-1	Particulate Debris Surrogate of the SiC Powder	11
Figure 3-2	Fiber Length Distribution.....	11
Figure 3-3	Chemical Powder.....	11
Figure 5-1	Pressure Drops vs. Particle to Fiber Ratio under a Hot-leg Break Condition.....	14

TS

ACRONYMS AND ABBREVIATIONS

BN	Bottom Nozzle
CCS	Containment Spray System
CL	Cold-Leg
dP	Differential Pressure
DVI	Direct Vessel Injection
ECCS	Emergency Core Cooling System
GSI	Generic Safety Issue
HL	Hot-Leg
HLSO	Hot-Leg Switchover
IRWST	In-containment Refueling Water Storage Tank
LOCA	Loss-Of-Coolant Accident
LTCC	Long-Term Core Cooling
NRC	United States Nuclear Regulatory Commission
P/F	Particle to Fiber
RCS	Reactor Coolant System
SG	Steam Generator
SI	Safety Injection
SiC	Silicon Carbide
T/C	Thermocouple

Page intentionally left blank

1 INTRODUCTION

The APR1400 containment building is designed to facilitate core cooling in the event of a postulated loss-of-coolant accident (LOCA). The cooling process requires water discharged from the break and containment spray to be collected in an in-containment refueling water storage tank (IRWST) sump for recirculation by the emergency core cooling system (ECCS) and the containment spray system (CSS).

Typically, an IRWST sump contains strainers in series that protect the ECCS components from debris washed into the sump. During ECCS recirculation operation following a LOCA event, the strainers collect fiber and particulates keeping them from being ingested into the ECCS and the CSS flow paths. Nonetheless, a portion of the particulates and fibrous material may still be ingested into the ECCS and, subsequently, into the reactor coolant system (RCS).

Concerns have been raised about the potential for debris ingested into the ECCS to collect on the fuel assembly and thereby affect long-term core cooling (LTCC) when recirculating coolant from the IRWST sump. This issue is collectively identified as United States Nuclear Regulatory Commission (NRC) generic safety issue (GSI)-191. To address this safety issue, in-vessel downstream effect tests were performed using a mock-up fuel assembly of the APR1400.

The objective of in-vessel effect tests is to obtain pressure drop data through a mock-up fuel assembly and to demonstrate that sufficient driving force is available to maintain an adequate flow rate to remove decay heat.

This report provides the test results of pressure drops through LOCA-generated debris deposited on a mock-up fuel assembly. Four tests were run to evaluate hot-leg break conditions with a four safety injection (SI) flow rate varying particle to fiber (P/F) ratios of []^{TS}. Seven tests were run to evaluate cold-leg break conditions with a core boil-off rate at 700 seconds after LOCA with varying P/F ratios of []^{TS}. Two types of tests using a two SI flow rate were performed to evaluate a hot-leg break with reduced SI condition and a cold-leg break after a hot-leg switchover (HLSO) operation condition.

The test results on pressure drops were compared with the available driving head in each LOCA scenario.

2 TEST FACILITY

A test facility was designed and constructed to measure the pressure drops across a mock-up fuel assembly. A schematic diagram of the test facility is shown in Figure 2-1, and a photo of the facility is shown in Figure 2-2. The test facility is composed of four main parts: a test column, a mixing tank system, a circulation system, and a control and monitoring system.

2.1 Test Column

The test column is composed of a mock-up fuel assembly in the test pool. The mock-up fuel assembly has a height of 2.5 m (8.2 ft) without fuel pellets, and is located on a simulated core support plate with a thickness of 30 mm (1.18 inch) and 70 mm (2.75 inch) flow holes. It includes top and bottom nozzles, a debris capturing fuel filter, top and bottom grids, four spacer grids, and 16 x 16 fuel rods. Pressure drops are measured at five points: the bottom nozzle (BN) and P-grid, the bottom grid, at four mid grids, at the top grid and top nozzle, and along the full length.

The test pool is made of transparent acrylic to be visible inside during the test. Water enters through a 40 mm (1.5 inch) nozzle at the bottom of the test pool and flows upward and exits through a 40 mm (1.5 inch) outlet at the top of the test pool. The bottom unit and top unit of the test pool excluding the fuel assembly region play the respective roles of the lower plenum and upper plenum of the reactor vessel. The water temperature in the test pool is measured by thermocouples (T/Cs) inserted through ports in the bottom and top.

2.2 Mixing Tank System

The mixing tank system is composed of a debris mixing tank and a chemical mixing tank. The debris mixing tank is manufactured as a transparent acrylic tank with a cylindrical shape, and it is capable of water suction in the downward vertical direction. A debris stirring tool is installed downward vertically at the top of the tank. A chiller piping and a heater are installed in the tank to control the water temperature. This heater is connected to a temperature control system, and the water temperature can be controlled from an environmental temperature of about 20 °C (68 °F) to a high temperature of 60 °C (140 °F).

A chemical mixing tank is installed on the upper part of the debris mixing tank to control the procedure of chemical surrogates addition to the test loop. It has a cylindrical shape with a 100 liter (26.4 gallon) volume and uses a chemical stirring tool.

2.3 Circulation System

The circulation system pumps water from the debris mixing tank, through the circulation piping and the test pool, and back into the debris mixing tank. A 1 kW pump draws water out of the bottom of the debris mixing tank. The flow rate is controlled by a control system with a computer. An electromagnetic flow meter measures the flow rate and provides feedback to the control system to maintain a constant flow rate.

2.4 Control and Monitoring System

The control system regulates the water flow rate and water temperature. The monitoring system records the differential pressure (dP), flow rate, and water temperature in the test pool and mixing tank. The measurement accuracy of the instruments is summarized in Table 2-1. The data can be recorded at a time interval chosen by the operator. The monitoring system is also used to check the slope of the dP versus time graph in order to evaluate whether the dP meets a steady state condition.

Table 2-1 Accuracy of the Measurement Instruments

TS



Figure 2-1 Schematic Diagram of the Test Facility

TS

Figure 2-2 Test Facility for the In-vessel Downstream Effect

3 TEST CONDITION

This test reflects the recirculation flow, temperature and debris conditions under the recirculation modes after a LOCA.

3.1 Flow Rates

3.1.1 Hot-leg Break

After a hot-leg (HL) break event, the maximum flow rate to the reactor vessel is expected to be 18,700 lpm (4,940 gpm) when all four SIs are available (Reference 1). Because the core bypass flow is not credited, all the SI water passes through the reactor core and exits the break location. Therefore, the flow rate per fuel assembly is calculated by dividing 18,700 lpm (4,940 gpm) by the number of fuel assemblies (241), giving a value of 77.6 lpm (20.5 gpm). The hot-leg break condition at the maximum flow rate was chosen to obtain the maximum pressure drop at the test column.

3.1.2 Cold-leg Break

In the event of a cold-leg (CL) break, most of the SI water spills directly out of the break location. The maximum SI flow rate to the core was selected as the core boil-off rate at the time of the start of recirculation. The SI flow rate per fuel assembly is 13.8 lpm (3.64 gpm) at the recirculation start time, which is around 700 seconds after a LOCA (Reference 1). For the conservative cold-leg break tests, a multiplier of 1.2 was applied, and the test flow rate was set to 16.6 lpm (4.38 gpm).

3.1.3 Cold-leg Break after a Hot-leg Switchover

Three hours after a cold-leg break, the operator starts a simultaneous hot-leg/direct vessel injection (DVI) line injection (hot-leg switchover: HLSO). Two SI pumps are for the hot-legs and two SI pumps are for the DVI lines. Because the water injected into the DVI lines spills directly out of the break location, the water injected into the hot-legs passes down through the reactor core toward the break location. Table 3-1 summarizes the SI flow rates per fuel assembly following a LOCA.

3.2 Water Chemistry and Temperature

Tap water was used to simulate the post-accident coolant. This is not representative of what would be expected for a LOCA. The coolant would contain a mixture of boric acid and trisodium phosphate at an elevated temperature. However, tap water and a low temperature were used in the tests because these conditions were expected to be conservative relative to actual reactor coolant conditions.

The water temperature was maintained at $22\text{ }^{\circ}\text{C} \pm 1\text{ }^{\circ}\text{C}$ ($71.6\text{ }^{\circ}\text{F} \pm 1.8\text{ }^{\circ}\text{F}$) during the tests. A lower water temperature covers post-LOCA core conditions because the water density is high at a low temperature, and the pressure drop increases at higher water density levels.

3.3 Debris Description

The circulating coolant may entrain debris that can be categorized as particulate, fiber, or chemical precipitates. The weight of latent debris is 90.7 kg (200 lbm), consisting of 83.9 kg (185 lbm) of particulate and 6.8 kg (15 lbm) of fiber in the APR1400 (Reference 1). All of the debris except for fiber transported to the sump was assumed to bypass the strainer. Because the number of fuel assemblies is 241 in the APR1400, the debris amount per fuel assembly was calculated by dividing the assumed amount of bypass debris by 241.

3.3.1 Particulate Debris

The Epoxy coatings are considered to be destroyed within the zone of influence in the containment. Based on an upstream analysis, the quantity of destroyed coating was 280.5 kg (618.4 lbm) (Reference 1). The NRC Safety Evaluation (Reference 2) estimated the particle size of failed coating to be 10 μm (0.4 mil) on average with a density of 1,505 kg/m^3 (94 lb/ft^3). A suitable and common surrogate is silicon carbide (SiC) with a mean particle size of 10 μm (0.4 mil) and a material specific gravity of 3.2, which corresponds to a density of 3,195 kg/m^3 (200 lb/ft^3). SiC was selected for its resistance to dissolution in tap water and for its interaction with other materials.

While the requirement for the characteristic size is 10 μm (0.4 mil) spheres, the SiC surrogate has a size distribution. This is actually quite conservative because it will create a higher packing density and create more drag and head loss in the debris bed. The maximum amount of SiC per fuel assembly is summarized in Table 3-2. Figure 3-1 shows a particulate debris surrogate of SiC powder.

3.3.2 Fibrous Debris

Fibrous insulation is not used in the zone of influence inside the containment of the APR1400. However, latent fiber is assumed, and the assumed quantity is 6.8 kg (15 lbm). The latent fiber is represented by NUKON[®] low density fiberglass with an as-fabricated density of 38.4 kg/m^3 (2.4 lb/ft^3) (Reference 2). The total strainer bypass fiber of the APR1400 was 1.67 kg (3.68 lbm) (Reference 1), and the mass of fiber per fuel assembly is summarized in Table 3-2.

For in-vessel downstream effect tests, the fiber length distribution specific to the APR1400 was measured using a Lorentzen and Wettre (L&W) Fiber Tester. A total of 164,328 fibers (60,100 fibers for filter bag number 21, and 104,228 fibers for filter bag number 29) were identified, with about 60% of the fibers less than or equal to 0.5 mm in length, 26% between 0.5 mm and 1 mm, and 14% greater than 1 mm (Table 3-3). The bypass fiber length distribution (Filter # 21, Filter # 29) is shown in Figure 3-2. The fiber length distribution for the APR1400 method was similar to that of the bypass fiber length distribution (Filter # 21, Filter # 29).

3.3.3 Chemical Precipitates

Based on the design conditions, the following chemical precipitates were available in the IRWST sump fluid of the APR1400 (Reference 1).

- Calcium phosphate: 0.7 kg (1.5 lbm)
- Sodium aluminum silicate: 4.3 kg (9.5 lbm)
- Aluminum oxyhydroxide (AIOOH): 180.1 kg (397 lbm)

Given the relative proportions, because AIOOH can be conservatively used to represent the other precipitates, only AIOOH was used in the test. The total chemical precipitate mass of 185.1 kg (408 lbm) was represented by AIOOH. The chemical precipitate was prepared in accordance with the WCAP-16530-NP (Reference 3) and was batched into the mixing tank in pre-defined quantities to collect the head loss data. This precipitate suspension has a calculated concentration of 11 grams per liter. The mass of AIOOH surrogate per fuel assembly is summarized in Table 3-2. Figure 3-3 shows the aluminum nitrate and sodium hydroxide prepared according to the WCAP-16530-NP.

3.4 Acceptance Bases for the Pressure Drop

It must be demonstrated that the available head to drive the SI flow into the core is greater than the head loss across the core due to possible debris buildup. The following relationship must hold to ensure that a sufficient flow is available to maintain the LTCC (Reference 4):

$$dP_{\text{avail}} > dP_{\text{debris}}$$

The available driving head (dP_{avail}) is a plant-specific value and the pressure drop due to debris (dP_{debris}) is determined by the in-vessel downstream effect test. The core flow is only possible if the manometric balance between the downcomer and the core is sufficient to overcome the flow losses in the core and loops at the appropriate flow rate.

$$dP_{avail} = dP_{dz} - (dP_{core} + dP_{loop})$$

Here, dP_{avail} is the total available driving head, dP_{dz} is the pressure head due to the liquid level between the downcomer and the core, and dP_{core} and dP_{loop} are the pressure heads due to flow losses in the core and loops, respectively. dP_{dz} was calculated using reactor vessel and steam generator drawing materials. dP_{core} and dP_{loop} were based on the values in LOCA analyses data (Reference 1).

When the available driving head under the hot-leg break condition was calculated, it was assumed that a siphon break occurs at the bottom of the steam generator (SG) tube sheet to account for the potential for voiding in the SG tubes. The available driving heads in each LOCA scenario are summarized in Table 3-4.

3.5 Test Matrix

The test matrix is described in Table 3-5. Two series of tests for hot-leg break and cold-leg break conditions were performed. [

] TS

Table 3-1 Flow Conditions in each LOCA Scenario

LOCA scenario	Core flow direction	APR1400 flow rate	Flow rate/ FA ⁽¹⁾	Remark
Hot-leg break	Upward	18,700 lpm (4,940 gpm)	77.6 lpm (20.5 gpm)	Maximum flow rate of four SI
Cold-leg break	Upward	3,322 lpm (880.2 gpm)	13.8 lpm (3.64 gpm)	Boil-off flow rate at 700 sec.
Cold-leg break after HLSO	Downward	9,350 lpm (2,470 gpm)	38.8 lpm (10.25 gpm)	Maximum flow rate of two SI

Note:

(1) 1/241 of the maximum flow rate

Table 3-2 Debris Types and Amounts per Fuel Assembly (FA)

Debris Type	Specific Type	Debris Generated in Containment	Assumed Bypass Debris (kg)	Per FA ⁽¹⁾ (g)
Fibrous	NUKON®	0	0	0
	Latent fiber	6.8 kg (15 lbm)	1.67 ⁽²⁾ (3.68 lbm)	6.93
Particulate	Coating debris	280.5 kg (3.1 ft ³)	280.5	1,164
	Latent particle	83.9 kg (185 lbm)	83.9	348
Chemical compounds		185.1 kg (408.0 lbm)	185.1	768 (70 liters)

Note:

(1) 1/241 of the assumed bypass debris amount

(2) Result of the APR1400 strainer bypass testing

Table 3-3 Fiber Length Distribution in Values

Length	Filter #21 (%)	Filter #29 (%)	APR1400 method (%)
Fiber length < 0.5 mm	58.4	60.0	65.4
0.5 mm ≤ Fiber length < 1.0 mm	26.7	26.0	17.0
1.0 mm ≤ Fiber length	14.9	14.0	17.6

Table 3-4 Available Driving Heads in each LOCA Scenario

LOCA scenario				
Hot-leg break				
Cold-leg break				
CL break after HLSO				

TS

Table 3-5 Test Matrix

TS

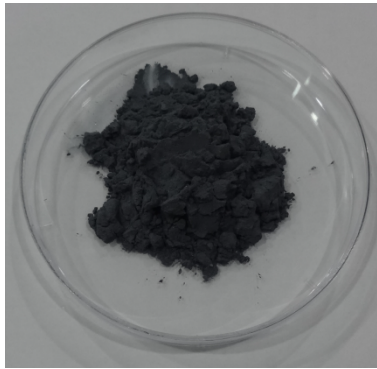


Figure 3-1 Particulate Debris Surrogate of the SiC Powder

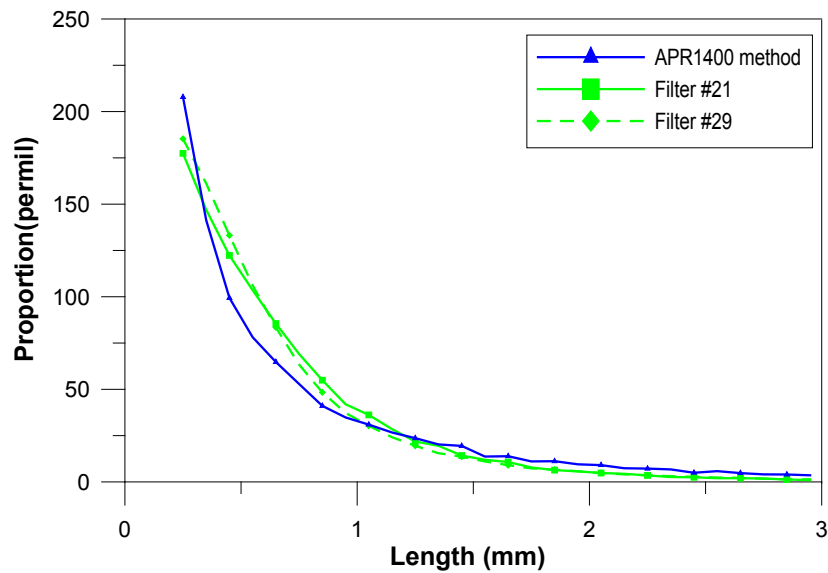


Figure 3-2 Fiber Length Distribution



(a) aluminum nitrate



(b) sodium hydroxide

Figure 3-3 Chemical Powder

4 TEST PROCEDURE

After the flow rate and water temperature were stabilized, debris was added in the sequence of particulate, fiber, and chemical surrogates.

4.1 Particulate Addition

- 1) Add the particulate debris to a 3 liter (0.8 gallon) vessel
- 2) Add 1 liter of the water (60 ~ 90 °C (140 ~ 194 °F)) to a 3 liter (0.8 gallon) vessel
- 3) Shake vigorously until the particulate material appears to be evenly dispersed in the solution
- 4) Pour the particulate slurry into the mixing tank
- 5) Rinse the vessel as much as necessary with the mixing tank solution
- 6) Allow the system to equilibrate for 1 loop volume turnover time

4.2 Fiber Addition

- 1) Add 3 g fiber to a 3 liter (0.8 gallon) vessel
- 2) Add 1 liter (0.26 gallon) of the water (60 ~ 90 °C (140 ~ 194 °F)) to each 3 liter (0.8 gallon) vessel
- 3) Shake vigorously until the fiber is well dispersed
- 4) Pour slowly the fiber suspension into the mixing tank
- 5) Rinse the 3 liter (0.8 gallon) vessel as much as necessary to remove the residual fiber
- 6) Wait for 1 loop volume turnover time
- 7) Repeat from Step 1 to Step 6 until all of the fiber has been added
- 8) Allow the system to equilibrate for 5 loop volume turnover time

4.3 Chemical Addition

- 1) Pour the AIOOH from the chemical makeup tank into the mixing tank in pre-defined increments as described in the test matrix
- 2) Allow the system to equilibrate for 3 loop volume turnovers for each addition
- 3) Record the time and the dP
- 4) Repeat from Step 1 to Step 3 until all of the AIOOH has been added

5 TEST RESULTS

TS

Table 5-1 Summary of the Test Results

TS

5.1 Hot-leg Break Tests

5.1.1 Summary of Hot-leg Break Tests

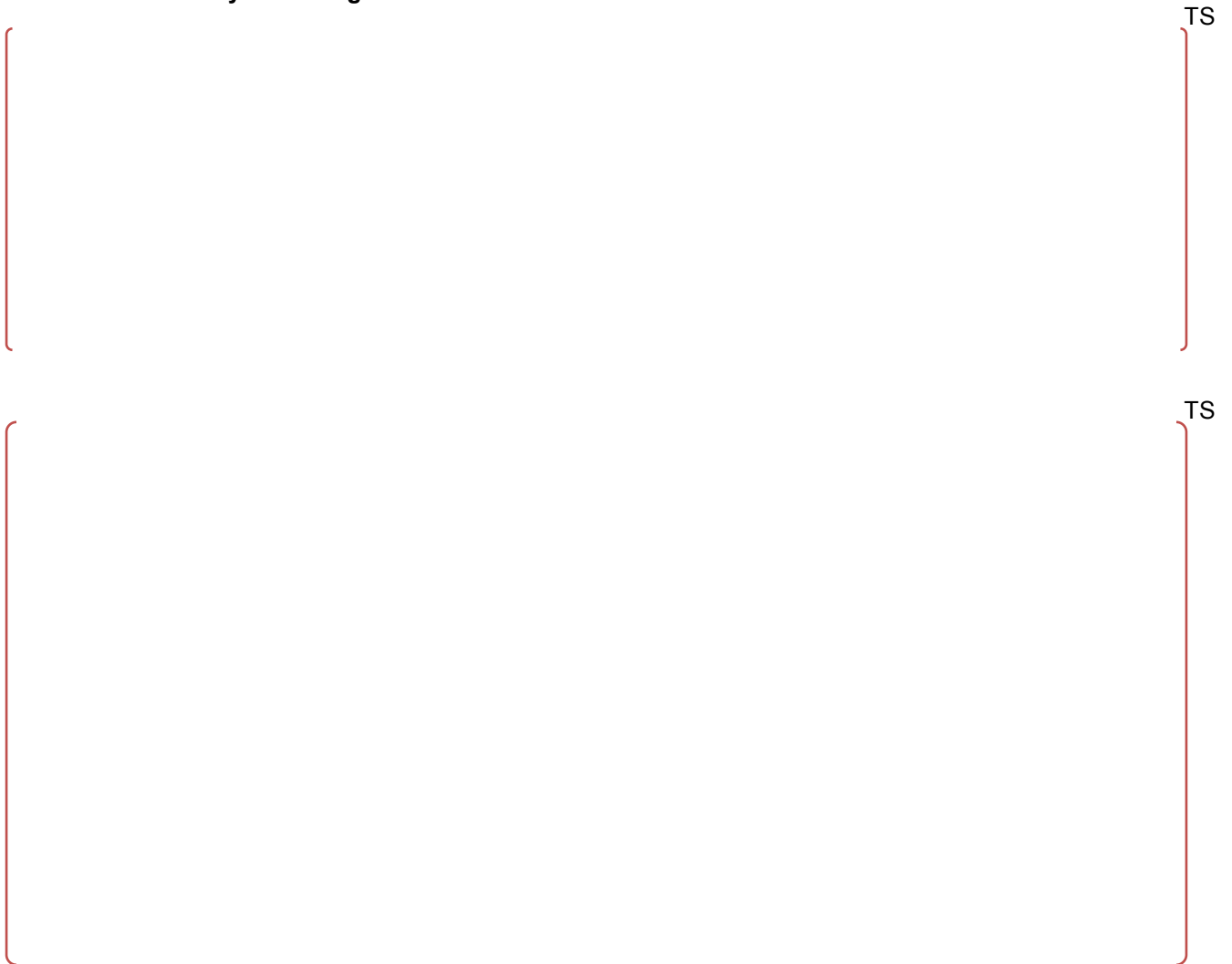


Figure 5-1 Pressure Drops vs. Particle to Fiber Ratio under a Hot-leg Break Condition

Test results will not be included in the non-proprietary version of this document.

5.2 Cold-leg Break Tests

5.2.1 Summary of Cold-leg Break Tests



Figure 5-13 Pressure Drops vs. Particle to Fiber Ratio under a Cold-leg Break Condition

Test results will not be included in the non-proprietary version of this document.

5.3 Cold-leg Break after a HLSO Test

5.3.1 Summary of Cold-leg Break after a HLSO Test

TS

Test results will not be included in the non-proprietary version of this document.

6 QUALITY ASSURANCE

This test was performed under the quality assurance program of the APR1400 (Reference 5) that satisfies 10 CFR part 50 Appendix B, 10 CFR Part 21, and ASME NQA-1-2008 and 1a-2009. All documents prepared and generated from this test were archived as QA records.

7 CONCLUSION

In-vessel downstream effect tests with a mock-up PLUS7 fuel assembly were performed to confirm that the head losses caused by debris meet the available driving head following a LOCA.

TS

Therefore, sufficient driving force is available to maintain an adequate flow rate to remove decay heat, and thus the LTCC capability is adequately maintained in the APR1400.

8 REFERENCES

1. APR1400-E-N-NR-14001-P, Rev. 0, "Design Features to Address GSI-191," KHNP, December 2014.
2. NEI 04-07, "Pressurized Water Reactor Sump Performance Evaluation Methodology," Nuclear Energy Institute, May 2004.
3. WCAP-16530-NP-A, "Evaluation of post-Accident Chemical Effects in Containment Sump Fluids to Support GSI-191," Westinghouse Electric Company LLC, March 2008.
4. WCAP-17057-NP, Rev. 1, "GSI-191 Fuel Assembly Test Report for PWROG," Westinghouse Electric Company LLC, September 2011.
5. APR1400-K-Q-TR-11005-NP, Rev. 4, "KHNP Quality Assurance Program Description (QAPD) for the APR1400 Design Certification," KHNP, March 2014.

APPENDIX A EFFECT OF A FLOW CHANNEL GAP CHANGE

Violation No. 99901453/2014-201-01(a)

The NRC requests that KHNP provide the evaluation for the impact of flow channel gap on the validity of testing in response to the NOV, under the inspection report number and project number, when that portion of the evaluation has been completed.

Response

This Appendix describes the impact of a flow channel gap on the validity of testing that has already been conducted to address in-vessel downstream effects of the APR1400.

A.1 Purpose

To simulate the arrangement of fuel assemblies (FAs) in the core, the gap between the mock-up fuel assembly and the test column was set to 1/2 of the distance between the fuel assemblies. However, the manufacturing tolerance in the gaps between the test column and the bottom nozzle resulted in some discrepancies compared to the design value.

This Appendix presents the test result of the most limiting condition with a re-manufactured test column, which meets the nominal value of the FA pitch and its tolerance (0.58 mm (0.023 inch) \pm 0.15 mm (0.006 inch)), as shown in Figure A.1-1.

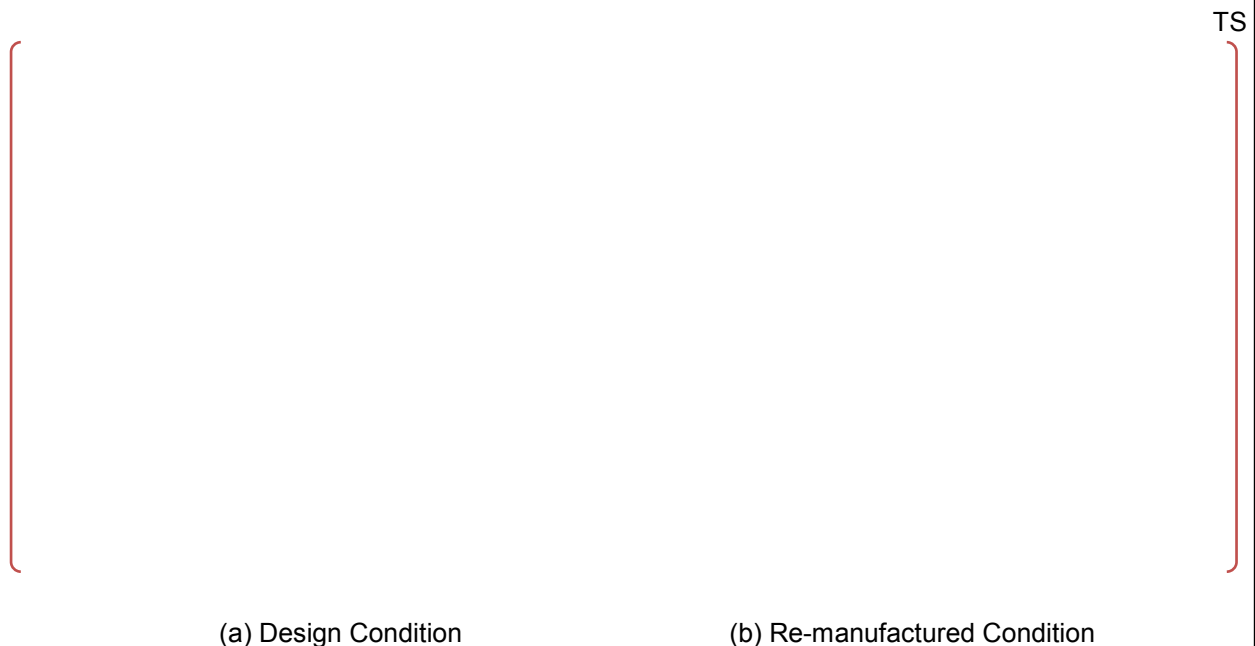


Figure A.1-1 Comparison of Gaps between Mock-up Fuel Assembly and Test Column (Unit: mm)

A.2 Sensitivity Test Results

A.2.1 Test Conditions

TS

A.3 Conclusion

A sensitivity test was conducted to assess the effect of a change in the gap size between the mock-up fuel assembly and the test column.

TS

Therefore, the results of test that have already been conducted are valid because there is a plenty of margin under the limiting condition of hot-leg break.

Table A.2-2 Test Sequence for APR1400-28

TS

TS

Figure A.2-1 Pressure Drops at P/F = 1 (APR1400-28)

APPENDIX B EFFECT OF DEBRIS SETTLING**Violation No. 99901453/2014-201-01(b)**

The NRC requests that KHNP provide the evaluation for the impact of debris settling on the validity of testing in response to the NOV, under the inspection report number and project number, when that portion of the evaluation has been completed.

Response

This Appendix describes the impact of debris settling on the validity of testing that has already been conducted to address in-vessel downstream effects of the APR1400.

B.1 Purpose

The phenomenon of debris settling was observed at the in-vessel effect tests of simulating cold-leg break. In this report, the applicability of the test results was evaluated by providing pressure drops through debris bed in which condition debris settling did not occur under the same particle to fiber (P/F) mass ratio.

B.2 Evaluation Method and Results**B.2.1 Conservatism in the Test Design**

Two conservative parameters were selected to cope with debris settling in the cold-leg (CL) break tests, as shown in Table B.2-1. The flow rate during the CL break tests was set to an increased value of 144% compared to the boil-off rate at 700 seconds after a loss-of-coolant accident (LOCA). The increased flow rate induces increased pressure drops, as shown in Figure B.2-1, and gives conservative test results.

The quantity of fibrous debris used in the tests was set to an increased value of 391% compared to the plant data. This implies that 74.4% of debris settling is allowed to simulate cold-leg break conditions.

In addition, debris settling at the structures and debris filtering at the sump strainers expected in the plant were not credited in the tests for conservatism.

B.2.2 Bounding Value of the Pressure Drop under the Cold-leg Break Tests

TS

B.3 Conclusion

TS

Table B.2-1 Conservatism in the Tests Considering Debris Settling

Parameter	APR1400 condition per fuel assembly	Tests condition	Remark
Flow rate during the CL break test	11.5 lpm	16.6 lpm	At 700 s after LOCA (144%)
Quantity of fibrous debris	3.83 g	15.0 g	Increased quantity (391%)

TS

TS

Figure B.2-2 Pressure Drops vs. Flow Rates at Different P/F Ratios

APPENDIX C ACCURACY OF THE GF630 FLOW METER**Violation No. 99901453/2014-201-03**

The NRC inspection team noted that the flow meter supplier's documentation stated that the flow measurements were not accurate in the low range used for the cold leg break tests. The NRC requests that KHNP provide more detail information as to how it was determined that the flow meter would provide accurate and repeatable information, when being used in a range the flow meter supplier's documentation indicated that it would not be accurate.

Response

This Appendix describes the accuracy and measurement range of the GF630 flow meter which was used in the in-vessel effect tests of the APR1400.

C.1 Purpose

The calibration range of the GF630 flow meter did not include the flow rate used in the cold-leg break tests when it was periodically calibrated in February of 2014. In this report, the evaluation of the recalibrated GF630 flow meter was performed to confirm that it meets the required accuracy in the measurement range (7.53 lpm to 250 lpm), as provided by the GF630 manufacturer Toshiba (Document No. EJL-140).

C.2 Results of the Evaluation

As shown in Figure C.2-1, the setting maximum flow rate of the GF630 is 15 m³/h (250 lpm). The requirements when checking the flow rate are also provided in Figure C.2-1, with a summary given in Table 2-1 (Section 2-4). The minimum measurement range of the GF630 is 0.4523 m³/h (7.54 lpm), as shown in Figure C.2-2.

The recalibrated certificate of the GF630 is shown in Figure C.2-3, and the evaluation result at the minimum flow rate is summarized in Table C.2-1. The deviations between the standard flow rate and the measured flow rate meet the requirement, and the repeatability of the measurement is maintained. Also, an adjustment of the GF630 is not necessary because it meets the requirements in the full measurement range.

TS

Thus, the target flow rate can be achieved because the control range is greater than the instrument uncertainty.

C.3 Conclusion

It was confirmed that the GF630 flow meter, which was used in the cold-leg break tests, met the required accuracy in the measurement range of 7.53 lpm to 250 lpm when it was recalibrated.

Therefore, it is concluded that the tests under the cold-leg break condition were performed with a flow meter which meets the required level of accuracy for in-vessel effect tests.

Table C.2-1 Evaluation of the GF630 Flow Meter at the Minimum Flow Rate

Standard flow rate(Y) (lpm)	Measured flow rate(X) (lpm)	Deviation (X-Y) (lpm)	Requirement (lpm)	Evaluation
7.748	7.91	0.162	0.25	Satisfactory
7.774	7.95	0.176	0.25	Satisfactory
7.362	7.52	0.158	0.25	Satisfactory

TOSHIBA
 TEST RECORD

	SUBJECT ELECTROMAGNETIC FLOWMETER	MFG.NO. 7219355 JL 0003C/0003D SERIAL NO. 116203297
--	---	--

DETECTOR SPEC.CODE	GF63004JFFA1	DETECTOR TAG.NO	—
CONVERTER SPEC.CODE	LF620AAA211F	CONVERTER TAG.NO	—
METER SIZE	40 mm	EXCITATION CURRENT	0.1370 A
SETTING MAX. FLOW	15 m ³ /h	SETTING FLOW VELOCITY	3.316 m/s
POWER SUPPLY VOLTAGE	AC100-240V	COUNT RATE	1 m ³ /p
H.ALM, HH.ALM	OFF (0%), OFF (0%)	L.ALM, LL.ALM	OFF (0%), OFF (0%)

 AMBIENT
 CONDITION
 26 °C
 36 % R H

Item	Requirements	Evaluation
Visual Check	The Appearance, lining, and construction, should be good.	<i>Satisfactory</i>
Resistance of detector against hydraulic pressure	Applying the static pressure of twice the flange standard to the detector for 15 minutes and check to make sure no water leakage occurs.	<i>Satisfactory</i>
Airtightness of detector and converter	No air leakage under 0.05 MPa air pressure during 1 minute.	<i>Satisfactory</i>
Isolation resistance of detector	50 MΩ or more at the following locations with DC 500V Megger. • Between electrode terminals (A,B) and frame ground. • Between excitation terminals (X,Y) and frame ground.	<i>Satisfactory</i> 1000MΩ
Isolation resistance of converter	50 MΩ or more at the following locations with DC 500V Megger. • Between Power supply terminals (L1,L2) and frame ground.	<i>Satisfactory</i> 1000MΩ
Dielectric strength of detector	AC 1500V at 1 minute between excitation terminal and frame ground.	<i>Satisfactory</i>
Dielectric strength of converter	AC 1500V at 1 minute between power supply terminal and frame ground.	<i>Satisfactory</i>
Operation test	Driving operation, warning circuit operation, display operation, and digital I/O functions must operate normally.	<i>Satisfactory</i>
The fluctuation of power supply voltage	The fluctuation of output should be less than ± 0.5% FS from AC 80V to AC 264V power supply.	<i>Satisfactory</i>
Checking of flow	±0.5% of rate in case of more than 20% of Max. flow ±0.1% FS in case of less than 20% of Max. flow	<i>Satisfactory</i>
Quantity check	The accessories agree with the purchase specifications.	<i>Satisfactory</i>

Figure C.2-1 Calibration Certificate of the GF630 Flow Meter According to the Supplier

TOSHIBA

Field Intelligent Device – Premium Value Series
Electromagnetic Flowmeter

GF630 /LF620
GF632 /LF622
15 to 900 mm (1/2" to 36")

Introduction

The electromagnetic flowmeter uses Faraday's Law of electromagnetic induction to measure the process flow. The device consists of two units: a detector, through which the fluid to be measured flows and in which low-level signals proportional to flow rates are obtained; and a converter, which supplies excitation current to the detector, and amplifies the signals from the detector and then processes and converts the signals into the 4–20mA dc current signal or communication signal. Combined with a multi-functional converter LF620 (combined type) or LF622 (separate type) equipped with its original patented noise-suppression circuit and advanced algorithms. The GF630 has a very high tolerance to noise, giving the unit a very stable output even for slurry fluid measurement. IR (Infrared) switches enable the parameter setting of the converter without removing the cover. Flow direction can be set in either way, and its unique 128 x 128 dot matrix LCD display allows the LCD to be rotated electronically to 90, 180 and 270 degrees without opening the cover. The terminal block in LCD side make easy to wire in case of the combined type.

The AF900 hand-held terminal (HART*¹ communicator) can be used to communicate with the flowmeter from a remote place. PROFIBUS-PA*² or Modbus*³ interface is available as an option.

*1: HART protocol (Highway Addressable Remote Transducer) is a communication protocol for industrial sensors recommended by the HCF (HART Communication Foundation).

*2: PROFIBUS is the communication protocol for factory and process automation that the PROFIBUS Organization recommends. Instead of analog control with a conventional analog signal (4–20mA), it is fieldbus which digitizes all signals. Flowmeters support PROFIBUS-PA.

*3: Modbus is the communication protocol that Modicon Inc. developed. Physical layer is RS485.

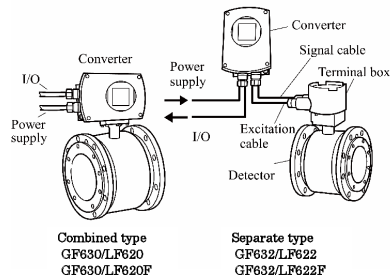


Figure 1. Configuration



Figure 2. GF630 Premium Value series Flowmeters



Certification
number
Z01207

Specifications

Overall Specifications

Measurement range in terms of flow velocity:

0–0.3 m/s to 0–10 m/s (0–1.0 ft/s to 0–32.8 ft/s).
0–0.1 m/s to 0–0.3 m/s (0–0.3 ft/s to 0–1.0 ft/s)
range is available optionally for meter size 1/2" to 18" (15 to 450 mm).

Accuracy:

<15mm to 450mm>

Pulse output:

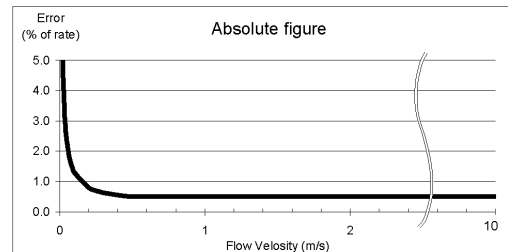
$V_s > 0.5$ m/s (1.64 ft/s): ± 0.5 % of rate.

$V_s < 0.5$ m/s (1.64 ft/s): ± 0.3 % of rate

± 1 mm/s (0.039 inch/s).

Current output: plus $\pm 8 \mu A$ (0.05 % of span)

Note: Span = Range in the magmeters.



Accuracy

EJL-140

Figure C.2-2 Specifications of the GF630 Flow Meter According to the Supplier (1/2)

GF630/LF620 GF632/LF622

Table 2. Flow Rate and Flow velocity (SI unit)

Unit: m³/h

Size (mm)	Flow rate				
	0.1 m/s	0.3 m/s	1.0 m/s	3 m/s	10 m/s
15	0.0636	0.1908	0.6361	1.908	6.361
25	0.1767	0.5301	1.767	5.301	17.67
32	0.2895	0.8686	2.895	8.686	28.95
40	0.4523	1.357	4.523	13.57	45.23
50	0.7067	2.120	7.067	21.20	70.67
65	1.195	3.583	11.95	35.83	119.5
80	1.809	5.428	18.09	54.28	180.9
100	2.827	8.482	28.27	84.82	282.7
125	4.417	13.25	44.17	132.5	441.7
150	6.361	19.08	63.61	190.8	636.1
200	11.31	33.93	113.1	339.3	1,131
250	17.67	53.01	176.7	530.1	1,767
300	25.45	76.34	254.5	763.4	2,545
350	34.64	103.9	346.4	1,039	3,464
400	45.23	135.7	452.3	1,357	4,523
450	57.25	171.7	572.5	1,717	5,725
500	—	212.1	706.9	2,121	7,069
600	—	305.4	1,018	3,054	10,180
700	—	415.6	1,385	4,156	13,850
750	—	477.1	1,590	4,771	15,900
800	—	542.9	1,810	5,429	18,100
900	—	687.1	2,290	6,871	22,900

Table 3. Flow Rate and Flow velocity (U.S. unit)

Unit: gal/min

Size (inch)	Flow rate				
	0.3ft/s	0.98ft/s	3ft/s	10ft/s	32.8ft/s
1/2'	0.2801	0.8403	2.561	8.532	28.01
1	0.7781	2.334	7.115	23.72	77.81
1 ¼	1.275	3.824	11.66	38.86	127.5
1 ½	1.992	5.975	18.21	60.71	199.2
2	3.112	9.337	28.46	94.86	311.2
2 ½	5.260	15.78	48.09	160.3	526.0
3	7.967	23.90	72.85	242.8	796.7
4	12.45	37.35	113.8	379.4	1,245
5	19.45	58.35	177.9	592.9	1,945
6	28.01	84.03	256.1	853.8	2,801
8	49.80	149.4	455.3	1,518	4,980
10	77.81	233.4	711.5	2,372	7,781
12	112.0	336.1	1,025	3,415	11,200
14	152.5	457.5	1,394	4,648	15,250
16	199.2	597.5	1,821	6,071	19,920
18	252.1	756.3	2,305	7,684	25,210
20	—	933.7	2,846	9,486	31,120
24	—	1,344	4,098	13,660	44,820
28	—	1,830	5,578	18,590	61,000
30	—	2,101	6,403	21,340	70,020
32	—	2,390	7,285	24,280	79,670
36	—	3,025	9,221	30,740	100,800

■ Calibration Range

If the calibration range is not specified, the standard range as shown below will be used. If the range is specified, we will use the specified range for calibration.


Table 4. Standard Flow Range

Meter size mm (inch)	Standard flow range			
	Flow rate (m ³ /h)	Flow velocity (m/s)	Flow rate (gal/min)	Flow velocity (ft/s)
15 (1/2)	2	3.144	25	29.283
25 (1)	6	3.395	75	31.625
32 (1 1/4)	10	3.454	125	32.171
40 (1 1/2)	15	3.316	175	28.826
50 (2)	25	3.537	300	31.625
65 (2 1/2)	40	3.348	475	29.629
80 (3)	60	3.316	650	26.766
100 (4)	100	3.537	1,000	26.354
125 (5)	150	3.395	1,750	31.625
150 (6)	200	3.144	2,500	29.283
200 (8)	300	2.653	4,500	29.649
250 (10)	600	3.395	7,000	29.517
300 (12)	900	3.537	10,000	28.283
350 (14)	1,200	3.465	12,000	25.817
400 (16)	1,600	3.537	16,000	26.354
450 (18)	2,500	4.366	20,000	26.029
500 (20)	3,000	4.244	25,000	26.354
600 (24)	4,000	3.930	40,000	29.283
700 (28)	5,000	3.609	50,000	26.892
750 (30)	6,000	3.773	60,000	28.112
800 (32)	7,000	3.868	70,000	28.825
900 (36)	8,000	3.930	80,000	26.029

Note: The unit of "gal/min" is not exchanged (converted) by "m³/h".

Figure C.2-2 Specifications of the GF630 Flow Meter According to the Supplier (2/2)


CALIBRATION CERTIFICATE

DAE DEOK HI-TECH CO., LTD. 94-17, Techno 2-ro, Yuseong-gu, Daejeon, Korea Tel : 042-936-8580, Fax : 042-936-8581	Certificate No. : 35211410 Page(1) of (2)																					
1. Client Name : KOREA HYDRO & NUCLEAR POWER Address : 71, 1312-gil, Yuseong-daero, Yuseong-gu, Daejeon																						
2. Calibration Subject Description : Electromagnetic Flowmeter Manufacturer and Model Name : TOSHIBA / 20AAA211F/GF63004JI Serial Number : 116203297																						
3. Date of Calibration : 2014. 10. 30.																						
4. Environment Temperature : (21.7 ± 0.2) °C Relative Humidity : (49 ± 2) % R.H. Location : <input checked="" type="checkbox"/> Permanent Calibration Lab <input type="checkbox"/> Mobile Lab <input type="checkbox"/> On Site Calibration																						
5. Traceability Calibration method and / or brief description The measuring instrument listed above was calibrated in accordance with the Standard Calibration Procedure of an Electro Magnetic Flow Meter for Liquid (DDH-CW-0103-080) using the Liquid standard flow measurement system that keep traceability from National Measurement Standard Institute. * List of used standards / specifications <table border="1" style="width: 100%; border-collapse: collapse; margin-top: 5px;"> <thead> <tr> <th>Description</th> <th>Manufacturer & Model</th> <th>Serial Number</th> <th>The due date of next Calibration</th> <th>Calibration laboratory</th> </tr> </thead> <tbody> <tr> <td>Mass Flowmeter</td> <td>E+H, Promass80F15</td> <td>9A04E102000</td> <td>2015. 3. 13.</td> <td>KRISS</td> </tr> <tr> <td>Electromagnetic Flowmeter</td> <td>SIEMENS, MAG 5100W/6000</td> <td>N1D8218235</td> <td>2015. 12. 24.</td> <td>K-water</td> </tr> <tr> <td>DVM</td> <td>HP, 34401A</td> <td>3146A37906</td> <td>2015. 1. 13.</td> <td>KRCMI</td> </tr> </tbody> </table>			Description	Manufacturer & Model	Serial Number	The due date of next Calibration	Calibration laboratory	Mass Flowmeter	E+H, Promass80F15	9A04E102000	2015. 3. 13.	KRISS	Electromagnetic Flowmeter	SIEMENS, MAG 5100W/6000	N1D8218235	2015. 12. 24.	K-water	DVM	HP, 34401A	3146A37906	2015. 1. 13.	KRCMI
Description	Manufacturer & Model	Serial Number	The due date of next Calibration	Calibration laboratory																		
Mass Flowmeter	E+H, Promass80F15	9A04E102000	2015. 3. 13.	KRISS																		
Electromagnetic Flowmeter	SIEMENS, MAG 5100W/6000	N1D8218235	2015. 12. 24.	K-water																		
DVM	HP, 34401A	3146A37906	2015. 1. 13.	KRCMI																		
6. Calibration result : Calibration result reference																						
7. Measurements Uncertainty : Calibration result reference																						
Affirmation	Measurements performed by Name : Seok-Jae Lee	Approved by Title : Technical Cal. Manager Name : Bong-Seok Shin																				
<p>The above calibration certificate is the accredited calibration items by Korea Laboratory Accreditation Scheme, which signed the ILAC-MRA.</p> <p style="text-align: right;">2014. 10. 31.</p> <p style="text-align: center; font-size: 1.2em;">DAE DEOK HI-TECH CO., LTD.</p> <p style="text-align: center;">Accredited by KOLAS, Republic of KOREA</p> <p>(NOTE) If any significant instability or other adverse factor(overload, temperature, humidity etc.) manifests itself before, during or after calibration, and is likely to affect the validity of the calibration,</p>																						

DDH-CP 양식 03-16 Rev. No.01

A4(210 mm × 297 mm)

Figure C.2-3 Calibration Certificate of the GF630 According to the KHNP Procedure (1/2)

CALIBRATION RESULT			Certificate No. : 35211410		
			Page(2) of (2)		
<p>Cal. Item : Electromagnetic Flowmeter Model No. : LF620AAA211F/GF63004JFFA1 Serial No. : 116203297 Cal. Date : 2014. 10. 30.</p>					
Standard Flow Rate(Y) (L/min)	Output Signal (mA)	Meter Flow Rate(X) (L/min)	Deviation (%)	Average Deviation (%)	Expanded Uncertainty (%)
248.248	19.842	247.53	-0.29		
249.202	19.892	248.31	-0.36	-0.33	0.28
247.870	19.808	247.00	-0.35		
190.900	16.180	190.31	-0.31		
189.442	16.094	188.97	-0.25	-0.31	0.28
191.543	16.215	190.86	-0.36		
127.883	12.157	127.45	-0.34		
130.205	12.308	129.80	-0.31	-0.33	0.28
130.704	12.337	130.26	-0.34		
68.433	8.368	68.24	-0.28		
69.182	8.424	69.12	-0.09	-0.18	0.28
70.362	8.496	70.25	-0.16		
7.748	4.506	7.91	2.10		
7.774	4.509	7.95	2.32	2.17	0.28
7.362	4.481	7.52	2.09		
<p>* Measured Fluid : Water * Meter size : 40 mm * Max Flow Range : 250 L/min * Signal Output : (4 ~ 20) mA * Deviation(%) = (X - Y) / Y × 100 * Meter Resolution : 0.01 L/min * The confidence level is about 95 %, k = 2 End.</p>					

DDH-CP 양식 03-16 Rev. No.01

A4(21) mm × 297 mm

Figure C.2-3 Calibration Certificate of the GF630 According to the KHNP Procedure (2/2)

APPENDIX D EFFECT OF BUBBLES IMPINGING ON THE BOTTOM NOZZLE**Violation No. 99901453/2014-201-04(b)**

The NRC requests that KHNP provide the evaluation for the impact of flow channel gap on the validity of testing in response to the NOV, under the inspection report number and project number, when that portion of the evaluation has been completed.

Response

This Appendix describes the impact of a flow channel gap on the validity of testing that has already been conducted to address in-vessel downstream effects of the APR1400.

D.1 Purpose

There is a procedure to remove air bubbles in the test loop before starting in-vessel effect tests. However, a few bubbles numbering from 4 to 7 with an approximate diameter of 5 mm were observed at the gaps between the bottom nozzle of the mock-up fuel assembly and the test column. This report describes the effect of bubbles in the test loop on the pressure drops qualitatively.

D.2 Results of the Evaluation

If air bubbles are present, there is a possibility of debris rupture when the air bubbles rise after the buildup of the debris bed. This phenomenon could have a negative effect on the pressure drops by the debris bed. However, the air bubbles in the test loop disappeared after the addition of particulate debris when there was no debris bed. Thus, the impact of bubbles impinging on the bottom nozzle of the fuel assembly is negligible.

Figure D.2-1 shows the comparison of the pressure drops between with air bubbles and without ones in the test loop. The green line is for the partially degassed case, and the blue line is for the fully degassed case. The dotted red line is the upper bound of uncertainty, which is obtained from the average value of blue line plus gauge uncertainty (0.064 kPa). All the particulates were added after 5 minutes from the beginning, and the system was allowed to equilibrate for 30 minutes. While the air bubbles were disappearing after the addition of particulates, any differences in the pressure drop trends were not found between the two curves.

D.3 Conclusion

Air bubbles in the test loop could have a negative effect on the pressure drops by the debris bed. However, as the air bubbles disappeared at the initial step of the tests, when there was no debris bed, the effect of air bubbles on the test results is negligible.

TS

Figure D.2-1 Comparison of Pressure Drops With and Without Bubbles in the Test Loop